Conducting polymerized high-internal-phase emulsion/single-walled carbon nanotube nanocomposite foams: Effect of the aqueous-phase surfactant type on the morphology and conductivity

Hossein Karimian,* Mohammad Reza Moghbeli

School of Chemical Engineering, Iran University of Science and Technology, Tehran 16846-13114, Iran
*Present address: School of Chemical Engineering, Golestan University, P.O. Box 45138-15739, Gorgan, Iran
Correspondence to: M. R. Moghbeli (E-mail: mr_moghbeli@iust.ac.ir)

ABSTRACT: Poly(styrene-*co*-divinylbenzene)/single-walled carbon nanotubes (SWCNTs) polymerized high-internal-phase emulsion (polyHIPE) nanocomposite foams were successfully synthesized with various types of aqueous-phase surfactants. The effects of anionic, cationic, nonionic, and mixed surfactants on the morphology and electrical conductivity of the resulting nanocomposite foams were investigated. The use of an anionic surfactant, sodium dodecylbenzesulfonate (SDBS), did not completely result in the typical polyHIPE nanocomposite foam microstructure because of the partial instability of the high-internal-phase emulsion. The nanocomposite foams synthesized by nonionic surfactants, that is, Pluronic F127 and Triton X-100, and the cationic/anionic mixture, cetyltrimethylammonium bromide/SDBS, exhibited the proper morphology, but the resulting nanocomposite foams were electrically insulators. Interestingly, the use of a Gemini-like surfactant, sodium dioctylsulfosuccinate (SDOSS), significantly improved both the typical morphology and electrical properties of the resulting nanocomposite foams because of the probable stronger interactions of SDOSS molecules with SWCNTs. The typical morphology of the nanocomposite foam synthesized with the SDOSS/F127 mixed surfactant was significantly improved, but the electrical conductivity decreased to some extent compared with the SDOSS-synthesized nanocomposite foams. This behavior was attributed to an increase in the tunneling length of the electrons between adjacent SWCNTs. © 2016 Wiley Periodicals, Inc. J. Appl. Polym. Sci. **2016**, *133*, 43883.

INTRODUCTION

Since their discovery by Iijima in 1991, carbon nanotubes (CNTs) have received much attention because of their extraordinary mechanical, thermal, and electrical properties.[1–9] The incorporation of small amounts of CNTs with high aspect ratios in polymeric matrices has brought about a new class of electrically conducting composite materials in which CNT networks form conducting paths.[10–14] Recently, some researchers have tried to disperse the relatively low contents of CNTs in high-internal-phase emulsions (HIPEs) to synthesize polymerized high-internal-phase emulsion (polyHIPE) nanocomposite foams with the aim of improving their mechanical and electrical properties.[15–18] As is well-known, HIPE is a specific water-in-oil (w/o) or oil-in-water concentrated emulsion with an internal phase volume ratio greater than 74%.[19] The internal phase of a typical w/o HIPE contains a water-soluble polymerization initiator, and the continuous phase consists of monomers and an emulsifier. The monomers in the continuous phase must be polymerized

to yield a typical porous interconnected open-cell foam with a low polymer volume fraction.[20] Because of the dispersion of CNTs in an interconnected open-cellular microstructure, the resulting polyHIPE nanocomposite foams with high specific surface areas are good candidates for use in the manufacturing of chemical sensors, absorbents, and electromagnetic interference (EMI) shields.[19–24] In addition, conducting nanocomposite foams as polymeric EMI shields have a very light weight compared to metal ones.

The use of stabilized nanoparticles in organic templates may also result in improved mechanical strength and electrical or thermal conductivity. Hermant *et al.*[15] used a two-step process to prepare polyHIPE/CNT nanocomposite foams. They used a polyelectrolyte to disperse single-walled carbon nanotubes (SWCNTs) into the aqueous phase of HIPEs, and then, the stabilized SWCNTs were added to the organic phase. The resulting composite foams were mainly closed-cell polyHIPEs with a limited number of cell interconnections and low electrical

conductivities close to 10^{-5} S/cm. As an alternative route, Hermant et al.[16] used sodium dodecyl sulfate (SDS) to disperse SWCNTs into the aqueous phase of HIPEs. The use of SDS [hydrophilic–lipophilic balance (HLB) = 40] for CNT dispersion significantly destabilized the w/o HIPEs and produced polyHIPE nanocomposite foams without a typical open-cell structure and proper mechanical properties. Menner et al.[17] prepared poly-HIPE nanocomposite foams with oxidized CNTs dispersed in the aqueous phase of the HIPEs. Their results show that the use of 4 wt % oxidized CNTs could improve the mechanical properties of the resulting nanocomposite foams, although they were electrically insulators. This behavior was connected to the good dispersion of CNTs in the polymeric matrix and the formation of grafted polymer layers on the surface of adjacent CNTs. The dispersion of relatively high CNT concentrations (1.7 wt %) in both the organic and aqueous phases of the HIPEs resulted in closed-cell polyHIPE foams with very low electrical conductivities.[17] The use of oxidized CNTs to stabilize medium-internal-phase emulsions led to polymerized medium-internal-phase emulsion nanocomposite foams with a closed-cell structure and very low electrical conductivities, despite the use of higher amounts of CNTs.[18] Although SWCNT dispersion can be improved by chemical functionalization, it can cause defects and reduces the electrical properties of nanotubes.[25] Therefore, CNTs are commonly dispersed by surfactants.
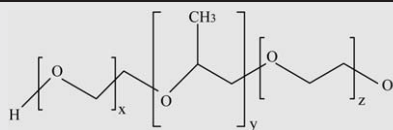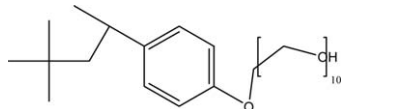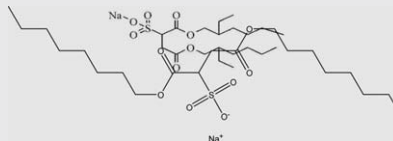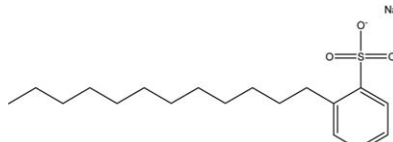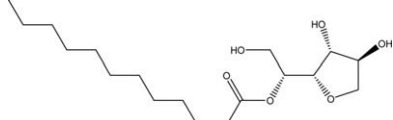
Although some investigations have been carried out to incorporate SWCNTs in the polyHIPE structure to obtain both the typical polyHIPE open-cell structure and high electrical conductivity, the achievement of one of the properties demolished the other property. Previous studies on polyHIPE/CNT nanocomposite foams have indicated that the main challenge has always been to achieve an interconnected open-cellular microstructure with a reasonable electrical conductivity.[15–18] In another words, strategies for obtaining such a microstructure with both improved mechanical and electrical properties have failed in most cases. Therefore, the achievement of the aforementioned important goal may provide us with the capability of using polyHIPE composite foams containing CNTs in devices requiring foams with improved morphological and electrical properties. In this research study, the effect of various surfactants, including anionic, cationic, and cationic/anionic mixed ones on the microstructure and electrical properties of poly(styrene-co-divinylbenzene)/SWCNT polyHIPE nanocomposite foams were investigated. For this purpose, SWCNTs were first dispersed in the aqueous phase of HIPEs with various surfactants. Thereafter, the SWCNT dispersions were added dropwise to the organic phase, and subsequently, the resulting HIPEs were polymerized to prepare solid nanocomposite foams. In addition, the effects of the surfactant type and SWCNT concentration on the electrical properties and microstructure of the nanocomposite foams were investigated.

EXPERIMENTAL

Materials
All of the chemical reagents were purchased from Merck Co. (Darmstadt, Germany) unless otherwise stated. Styrene and divinylbenzene were distilled in vacuo to remove traces of

Table I. Chemical Structures of the Dispersing Agents

Dispersing agent	Structure
Pluronic F127 (x = 100, y = 65, z = 100)	
Triton X-100	
SDOSS	
SDBS	
CTAB	
Span20	

inhibitor and stored at 5 °C before use. Sorbitan monooleate (Span80), sorbitan monolaurate (Span20), and azobisisobutyronitrile were used without any further purification. SWCNTs (ArkNano, China) with an average length of 30 μm and an average diameter of 2 nm were used as conducting nanofillers. Sodium dodecylbenzesulfonate (SDBS), cetyltrimethylammonium bromide (CTAB), sodium dioctylsulfosuccinate (SDOSS), Triton X-100, and Pluronic F127 were used as dispersing agents. The chemical structures of the agents used for SWCNT dispersion are listed in Table I. Deionized distilled water (DDI) was prepared in our laboratory.

Preparation and Characterization of Colloidal SWCNT Dispersions
The SWCNTs were dispersed well in the aqueous phase of HIPEs with a horn sonicator (Bandelin, Germany). Aqueous dispersions with various SWCNT contents were prepared with certain amounts of various surfactants. The sonication power was maintained at 30 W during the exfoliation for 1 h, whereas the dispersion was placed in an ice bath to reduce SWCNT damage. After sonication, the dispersion was diluted 100 times with DDI for ultraviolet–visible (UV–vis) spectroscopy. The absorbance peaks of the samples were recorded on a UV–vis spectrophotometer (PerkinElmer). Blank samples were prepared with an appropriate amount of surfactants in DDI.
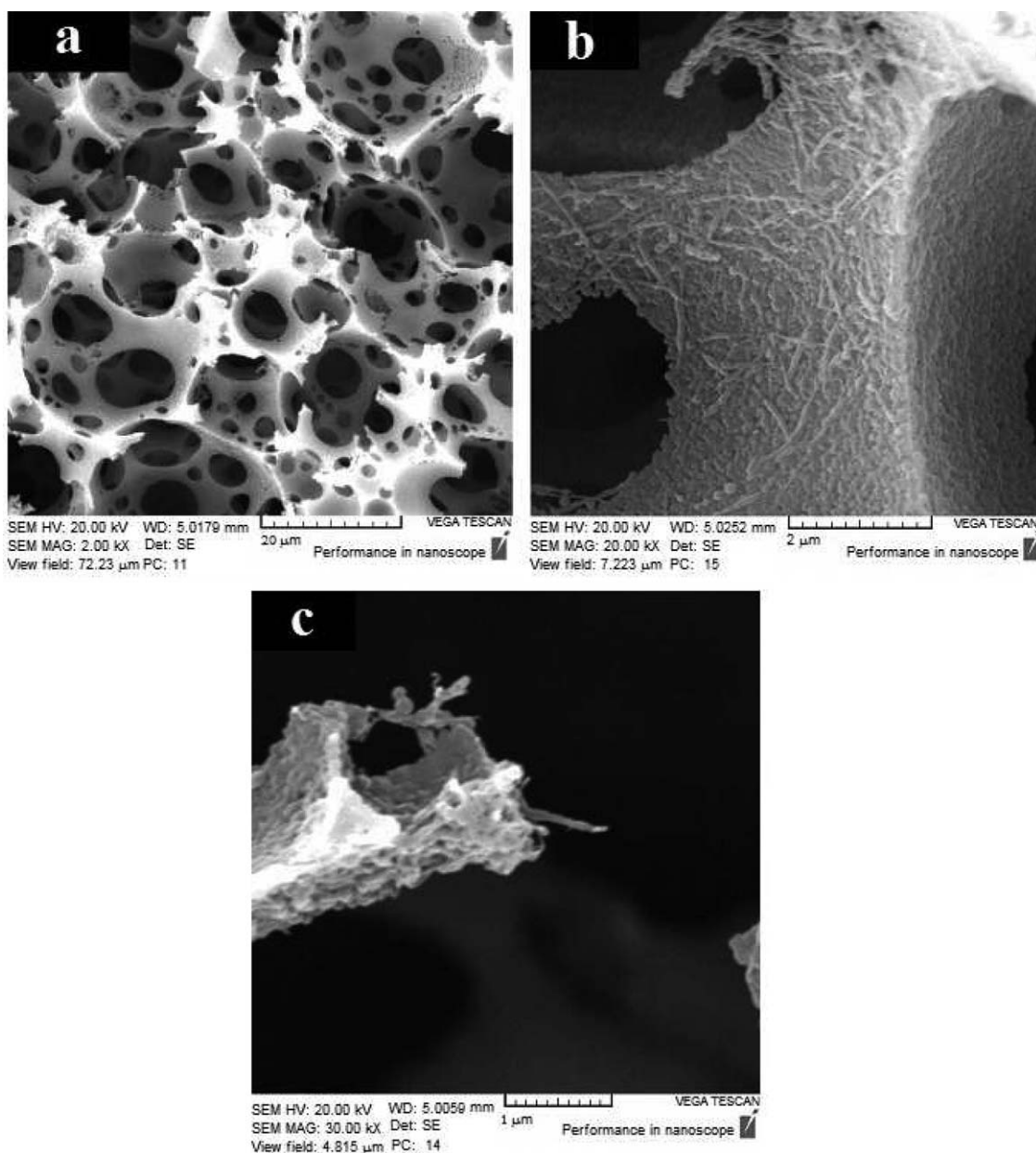
Figure 1. SEM micrographs of the polyHIPE nanocomposite foam containing 0.3 wt % SWCNTs prepared with Triton X-100.

Preparation of the PolyHIPE Nanocomposite Foams

The aqueous phase of HIPE (85 vol %) containing various amounts of SWCNTs (0–1 wt %) was added dropwise to the organic continuous phase. The organic phase consisted of styrene, divinylbenzene (styrene/divinylbenzene = 1/1 v/v), 20 vol % Span80, and 1 mol % azobisisobutyronitrile on the basis of the total monomers. In the case where the cationic/anionic surfactant system was used to prepare nanocomposite foams, the aqueous phase consisted of SWCNTs dispersed by 0.4 wt % SDBS, whereas the organic phase consisted of 6.3 wt % Span20 and 0.3 wt % CTAB, all on the basis of the total monomers. The emulsification process was carried out with a mechanical overhead stirrer (Heidolph, Germany) at 700 rpm and room temperature. The concentrated emulsions, HIPEs, were then transferred into glass molds and polymerized after they were sealed at 60 °C in a circulating oven for 24 h. The polymerized emulsions were then dried at 70 °C for a further 24 h. A similar procedure was used to prepare neat polyHIPE solid foams without any SWCNTs. In this case, for comparison purposes, the aqueous phase consisted of DDI and dispersing agents in the absence of SWCNTs.

Foam Characteristics

Morphology and SWCNT Dispersion. The morphology of polyHIPE foams was studied by scanning electron microscopy (SEM, WEGA/TESCAN, Czech Republic) and field emission scanning electron microscopy (FESEM, Hitachi S-4160, Japan). The polyHIPE foams were first fractured in liquid nitrogen. Thereafter, the fracture surface was coated with a thin layer of gold before SEM observation. The mean size of the cells and
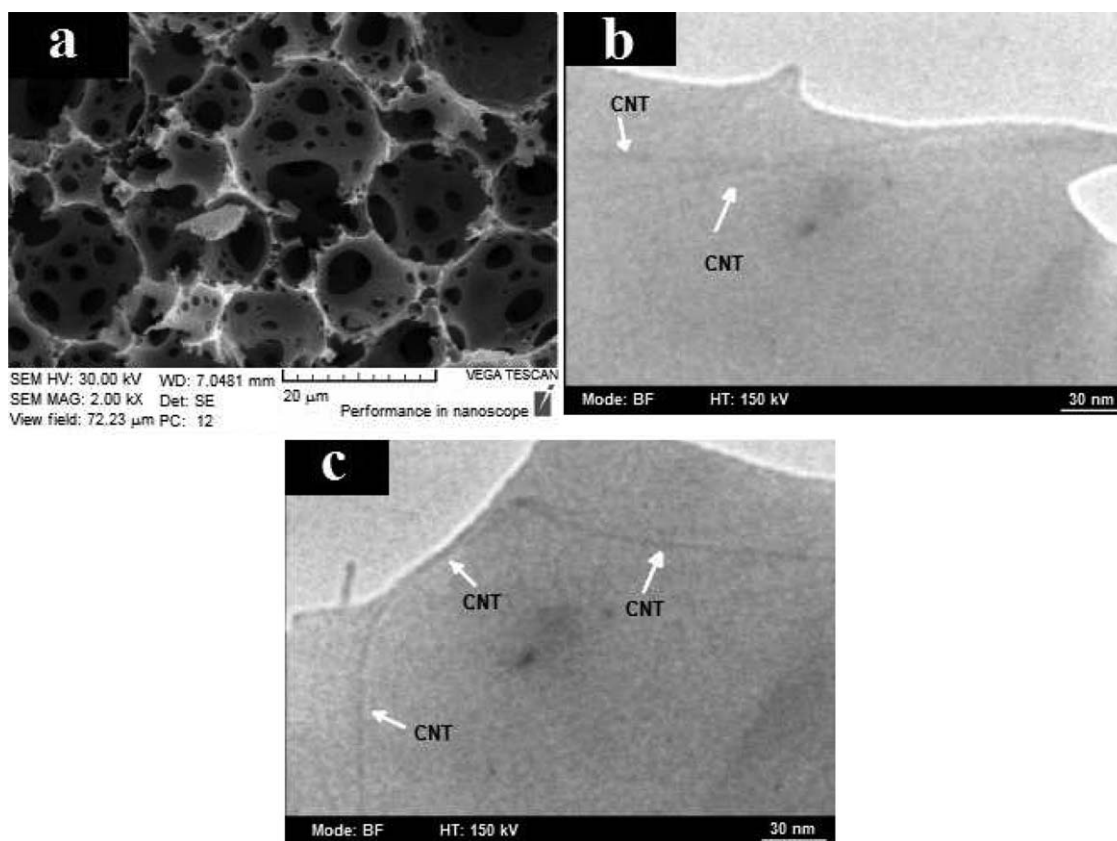
Figure 2. (a) SEM and (b,c) TEM micrographs of the polyHIPE nanocomposite foam containing 0.3 wt % SWCNTs prepared with F127.

windows was calculated approximately from the SEM micrographs of 100 cells or windows with the following equations[26]:

$$\bar{D}_n = \frac{\sum_i N_i D_i}{\sum_i N_i} \tag{1}$$

$$\bar{D}_w = \left[\frac{\sum_i N_i D_i^6}{\sum_i N_i D_i^3}\right]^{1/3} \tag{2}$$

where $\bar{D}_n$ and $\bar{D}_w$ are the number-average and weight-average cell sizes, respectively, and N_i is the number of cells or windows with a diameter of D_i. The polydispersity index (PDI) is a criterion of the cell or window size distribution within the polymeric foam.[26]

The dispersion state of the SWCNTs was investigated by transmission electron microscopy (TEM; Philips, The Netherlands). For this purpose, the porous nanocomposite foams were filled by an epoxy resin, and after the resin was cured, the samples were used to prepare suitable thin slices for microscopic observation. TEM micrographs were taken from ultrathin polyHIPE slices prepared by an ultramicrotome device with a diamond knife. The cut slices were put on 400-mesh copper grids and dried for 2 h at room temperature before microscopy.

Electrical Conductivity Measurement. A thin slab $(1 \times 1 \times 0.4 \text{ cm}^3)$ was cut from the prepared nanocomposite foams for electrical conductivity measurements. Two flat edges of the slabs were painted with silver paste to adhere thin copper sheets to the edges. The copper sheets act as two electrodes for subsequent two-point direct-current conductivity measurements.

RESULTS AND DISCUSSION

For conducting polyHIPE/CNTs foams, the microstructure of final nanocomposite foams should be preserved by the addition of CNTs to HIPEs. However, the use of water-soluble emulsifiers to disperse CNTs in the aqueous phase often leads to an unstable HIPE and, consequently, to polyHIPE nanocomposite foams losing their typical microstructure and conductivity.[15–18] Accordingly, the goal of this study was to achieve polyHIPE/SWCNT nanocomposite foams with an interconnected open-cellular microstructure and reasonable electrical conductivity with a suitable surfactant or surfactant mixture. In this study, common anionic, cationic, and mixed surfactants were used to disperse SWCNTs in the aqueous media of foam emulsions. To select the proper surfactants, the HLB and chemical structure of the surfactants were considered.

Nonionic Surfactants

To investigate the effect of nonionic surfactants on the microstructure and electrical conductivity of the polyHIPE nanocomposite foams, SWCNTs were exfoliated in the aqueous phase of the HIPEs with Pluronic F127 (HLB for F127 = 22) and Triton X-100 (HLB for Triton = 13.5). Figures 1(a) and 2(a) show the SEM micrographs of the nanocomposite foams containing 0.3 wt % SWCNTs prepared by Triton X-100 and F127, respectively. As shown, the typical open-cell polyHIPE structure was

43883 (4 of 12)   *J. APPL. POLYM. SCI.* **2016**, DOI: 10.1002/APP.43883

Table II. Mean Cell and Pore Sizes of PolyHIPE Foams Prepared with Different Surfactants

Surfactant	SWCNTs (wt %)	Cells			Windows		
		D_n (nm)	D_w (nm)	PDI (nm)	D_n (nm)	D_w (nm)	PDI (nm)
F127	0	19.94	22.91	1.15	3.32	4.54	1.36
F127	0.3	11.98	15.14	1.26	2.91	4.48	1.54
Triton X-100	0.3	17.67	21.73	1.23	6.97	3.92	1.78
SDBS/CTAB/Span20	0.0	25.15	66.48	2.64	6.26	5.12	1.34
	0.05	13.09	16.23	1.24	3.81	5.12	1.34
	0.2	10.88	11.49	1.06	2.23	2.53	1.15
	0.4	8.77	9.68	1.12	2.06	2.63	1.27
SDBS	0.3	7.32	7.93	1.08	1.97	2.15	1.09
SDOSS	0	12.01	12.95	1.08	3.58	4.15	1.16
SDOSS	0.3	8.95	9.89	1.1	2.85	3.19	1.11
SDOSS	1	5.38	5.63	1.05	1.41	1.52	1.08
SDOSS/F127	0.3	11.5	12.32	1.07	3.39	4.25	1.25
SDOSS/F127	1	10.43	10.91	1.05	2.99	4.23	1.41

observed for both nanocomposite foams because of the effective role of the nonionic surfactants in dispersing SWCNTs in the aqueous phase of the HIPEs. Because of the high HLB values of the surfactants, we expected that the surfactants destabilized the HIPEs, such as those prepared with the anionic one, that is, SDBS (HLB for SDBS = 11.8). Nonetheless, the emulsions remained stable, and thereby, the composite foams showed the typical interconnected open-cell polyHIPE microstructure. The lack of spherical particles on the polyHIPE walls prepared with F127 and Triton X-100 were attributed to the higher stability of the HIPEs and the lack of formation of local oil-in-water emulsions in the aqueous phase.

We concluded that HLB was not the only crucial factor determining the type of suitable surfactant for both CNT dispersion and HIPE stabilization, but the chemical structure of surfactant was also of great importance. Pluronic F127 was a triblock copolymer of ethylene oxide and propylene oxide with a molecular weight of 12,800 g/mol, whereas Triton X-100 was a nonionic surfactant with a molecular weight of 625 g/mol synthesized through polymerization of octylphenyl with ethylene oxide. In the case of F127, the poly(propylene oxide) (PPO) blocks seemed to engulf the surface of SWCNTs, whereas the poly(ethylene oxide) (PEO) blocks were oriented in the aqueous phase to prevent SWCNT agglomeration through steric repulsion.[27]

The poor coverage of the SWCNT surfaces may have led to agglomeration because of the attractive van der Waals forces between the bare surfaces of the SWCNTs through bridging mechanism in which a polymeric chain could be attracted to two or more nanotubes simultaneously. In addition, the copolymer chains should be hung so they cannot be removed from the SWCNT surfaces while randomly moving in the aqueous phase. Therefore, F127 is suitable for this purpose because its PEO blocks are more soluble in the aqueous phase, whereas the

PPO blocks tend to be attracted to the surface of SWCNTs.[27] In addition, the thickness of the adsorbed layer should be adequate for the development of effective steric interactions between the SWCNTs covered by the copolymer. The PEO blocks with a molecular weight of 4400 g/mol and an approximate segment length of 25 nm seemed to be suitable for full stretching.

For the nanocomposite foam prepared with Triton X-100, an interconnected open-cellular structure was observed [Figure 1(a)]. The voluminous phenyl group of Triton X-100 may have improved the stability of HIPE through steric interactions. The SEM micrograph of the nanocomposite foam indicated the formation of a SWCNT network on the void walls of the foam [Figure 1(b)]. Some SWCNTs were pinned out of the fracture cross section [Figure 1(c)]; this represented the diffusion of stabilized SWCNTs from the aqueous phase into the organic phase during polymerization due to the changes in their hydrophilicity. Despite the contact of the adjacent SWCNTs on the foam surface, the thickness of the insulating copolymer layer on the nanotubes seemed to be greater than the electron tunneling length; this prevented the electron transport between the adjacent nanotubes.[28]

However, the nanocomposite foams prepared with F127 and Triton X-100 were electrical insulators. The thickness of the insulating layer formed by the polymeric matrix on the SWCNT surface was greater than the tunneling length of the electrons.[28] TEM micrographs of the nanocomposite foam prepared by F127 [Figure 2(b,c)] confirmed that the arrangement of the SWCNTs in the organic phase near the void wall surface prevented coalescence of the water droplets in the HIPE through Ostwald ripening. In addition, the presence of bulky molecules of the block copolymer around SWCNTs resulted in the larger distance of SWCNTs and led to increased noncontact resistance between the conducting nanofillers. Although the SWCNTs were dispersed into the aqueous phase, the tubes were mainly observed within the void wall rather than on its surface [Figure
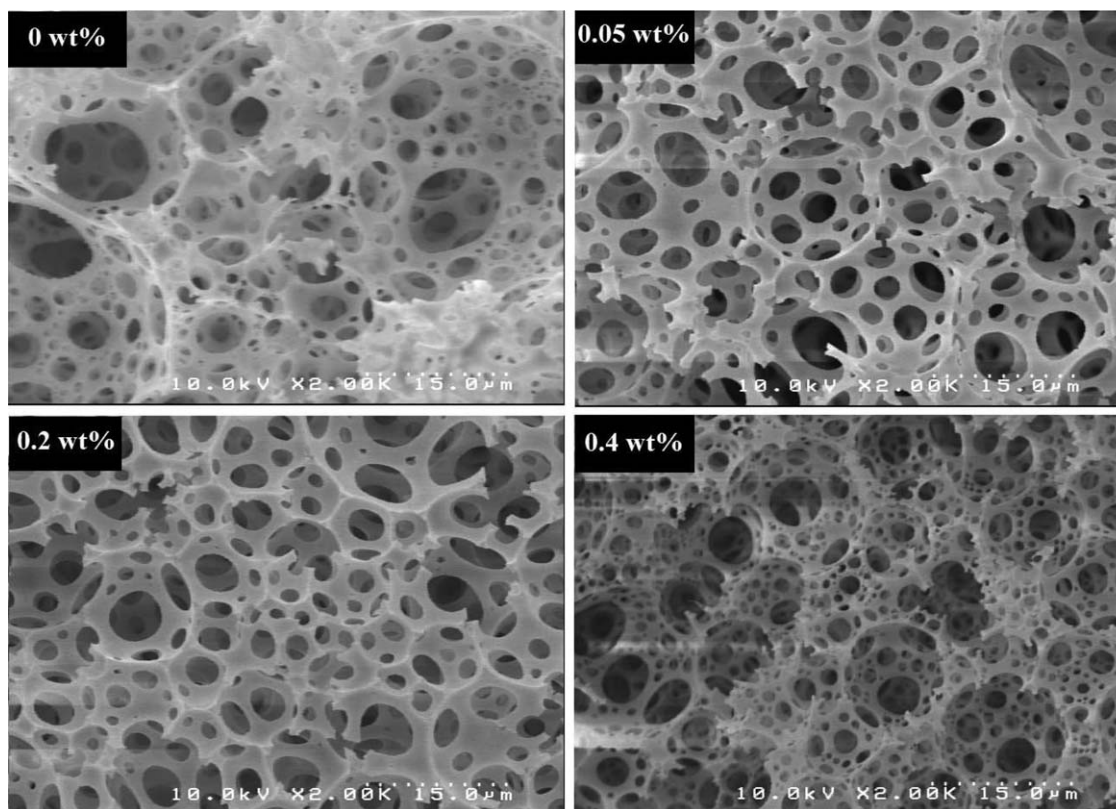
Figure 3. FESEM micrographs of polyHIPE nanocomposite foams prepared with a SDBS/CTAB/Span20 mixed surfactant containing various amounts of SWCNTs.

2(b)]. Furthermore, polymer grafting may have occurred on the surface of the SWCNTs to increase the hydrophobic nature of the SWCNTs and lead to nanotube diffusion in the organic phase. Partial separation of the surfactant molecules from the SWCNT surface may have increased their probable migration to the organic phase.

Table II shows the mean cell and window size of the nanocomposite foams. The incorporation of 0.3 wt % SWCNTs in the neat polyHIPE foam decreased the mean size of voids and windows by 40 and 12%, respectively. These changes were attributed to the role of CNTs as a barrier at the interface between the phases; this suppressed the phenomena and led to HIPE instability. In addition, the higher efficiency of the aforementioned nonionic surfactants reduced Ostwald ripening and coalescence of the aqueous droplets.

Despite the good morphological characteristics of the nanocomposite foams prepared by the nonionic surfactants, the resulting foams were electrical insulators. Accordingly, alternative approaches were used to achieve foams with both an interconnected open-cell structure and proper electrical conductivity with high-efficiency surfactant mixtures.[29] For this purpose, the nanocomposite foams were prepared with mixtures of surfactants to disperse SWCNTs in the HIPEs.

Cationic/Anionic Mixed Surfactant

To prepare nanocomposite foams, a mixture of anionic, SDBS, cationic, CTAB, and the nonionic Span20 surfactants were used

to disperse 0.05, 0.2, and 0.4 wt % SWCNTs in the HIPEs. Figure 3 shows the SEM micrographs of the resulting nanocomposite foams prepared with the mixed-surfactant system. As shown, all of the foams resembled the open-cell microstructure of the polyHIPE foams. In fact, a mixture of cationic or ionic surfactant with an amphiphilic one increased the stability of the concentrated emulsions. The interfacial film developed by the mixture of surfactants resisted the pressure caused by droplet contact and, consequently, prevented Ostwald ripening.[29]

Table II summarizes the mean cell and window diameters of the nanocomposite foams. As seen, the mean cell and window size decreased with increasing SWCNT content in the aqueous phase of the HIPEs. It appeared that the presence of SWCNTs increased the stability of emulsions and led to polyHIPE foams with smaller cells.[15] During the dispersion, the anionic and cationic surfactants could be physically adsorbed on the surface of the SWCNTs and could stabilize the nanotubes in the aqueous phase. The SWCNTs stabilized by the SDBS/CTAB mixture created a rigid barrier against the diffusion of dispersed droplets with the help of the nonionic surfactant Span20. As a result, droplet growth through coalescence and Ostwald ripening was prevented.[29] Despite their good morphological properties, the foams prepared with the surfactant mixture were electrical insulators; this was presumably due to the good dispersion of SWCNTs in the polymeric matrix and the formation of an insulating polymeric layer around the nanotubes.[17] The insulating layer may have prevented the effective electrical contact of the
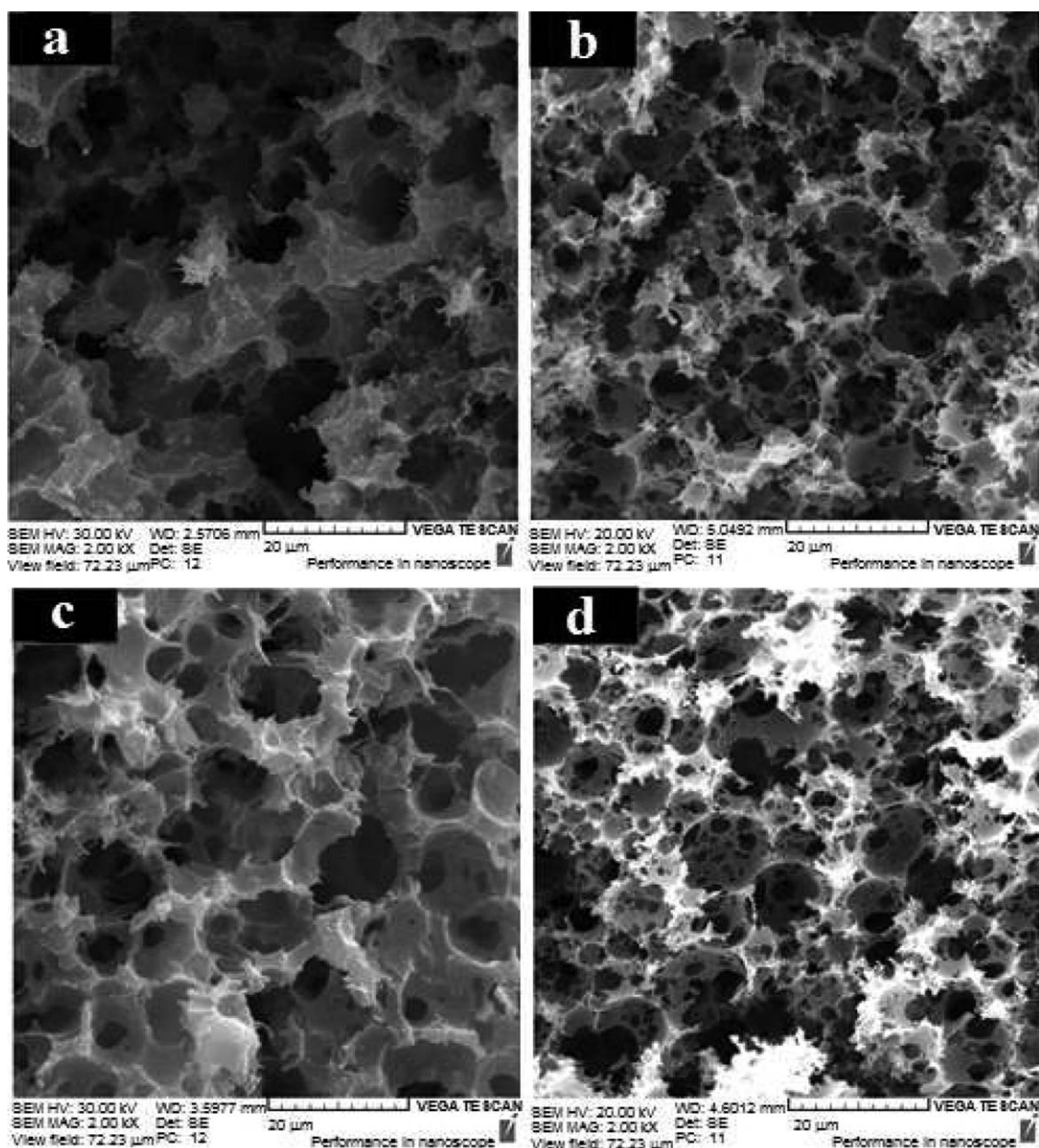
Figure 4. SEM micrographs of polyHIPE nanocomposite foams prepared with different surfactants and SWCNT levels: (a) SDBS and 0 wt % SWCNTs, (b) SDBS and 0.3 wt % SWCNTs, (c) SDOSS and 0 wt % SWCNTs, and (d) SDOSS and 0.3 wt % SWCNTs.

SWCNTs to form conducting networks. The use of a surfactant mixture containing an anionic surfactant with a suitable chemical structure and another one with a block copolymer structure seemed to be effective in the stabilization of the SWCNT dispersions.[30] In the next section, an anionic surfactant, that is, SDOSS, and its mixture with Pluronic F127 were used to prepare nanocomposite foams containing various amounts of SWCNTs.

Effect of SDOSS on Nanocomposite Foam Properties

To synthesize nanocomposite foams, the aqueous phase of HIPEs containing SWCNTs was prepared with a certain amount of SDOSS with an ultrasound homogenizer. Figure 4 shows the SEM micrographs of the neat polyHIPE foam and its composite

with 0.3 wt % SWCNTs. SDBS was also used to prepare foams with the same SWCNT loadings for comparison purposes. The SEM micrographs indicate a significant improvement in the foam microstructure with the SDOSS surfactant; this resulted in a distinguishable typical polyHIPE morphology as compared with that prepared with SDBS one.

This behavior was attributed to the chemical structure of the surfactants used for the dispersal of SWCNTs in the aqueous phase (Table I). For effective dispersion, the surfactant molecules should form stable micellar structures around the CNTs to overcome strong attractive forces induced by π bonds. In addition, the surfactant should contain a long and, preferentially, an irregular tail to suspend long and rigid CNTs through the
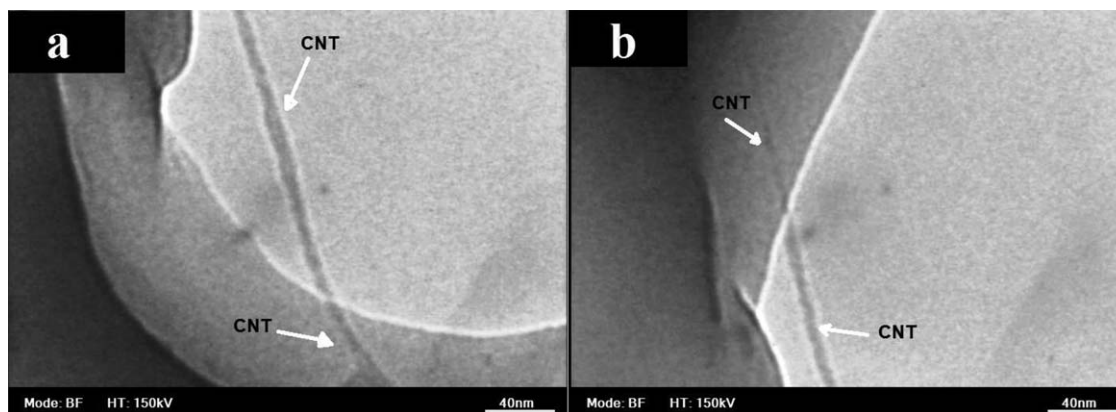
Figure 5. TEM micrographs of a polyHIPE nanocomposite foam containing 0.3 wt % SWCNTs dispersed by an SDOSS surfactant.

creation of a large solvation shell around CNTs. If the surfactant tail is electrically charged, the columbic repulsion will prevent CNTs from agglomerating.[31] Most studies have used SDS for the dispersion of CNTs.[21] However, the literature suggests that the higher performance of SDBS compared to SDS to stabilize and disperse CNTs in aqueous media is presumably due to the special π–π interactions created between the CNTs and aromatic ring of SDBS.[31,32]

However, among the anionic surfactants, SDOSS, SDS, and SDBS, the former outperformed SDS and SDBS in terms of the dispersion of CNTs in the aqueous solutions.[31] This was connected to the irregular branched tail of SDOSS compared with the linear alkyl tails of SDS and SDBS and leads to a larger solvation shell around SWCNTs. Thus, the nanocomposite foams prepared with SDOSS showed a more regular polyHIPE microstructure because of the higher HIPE stability [Figure 4(c,d)].

Interestingly, the chemical structure of SDOSS was fairly similar to those of Gemini surfactants with more than one hydrophobic tail and a hydrophilic head (Table I). Gemini surfactants have a much lower lower critical micelle concentration than common surfactants. In addition, the properties of Gemini surfactants are strongly dependent on the structure and length of the spacer that separates the surfactant tails.[31] Hence, the Gemini-like surfactants, such as SDOSS, were expected to have different interactions with SWNCTs compared with common surfactants. The higher performance of SDOSS in improving poly(styrene-*co*-divinylbenzene)/SWCNT polyHIPE morphology (Figure 4) was attributed to stronger adsorption and more compact arrangement of the hydrophobic tail on the surface of SWCNTs. SDOSS with two alkyl chains caused stronger hydrophobic interactions with SWCNTs. Thus, few adsorbed SDOSS molecules (HLB = 32) may have migrated to the aqueous phase during the polymerization process. The higher stability of HIPEs in the presence of SDOSS molecules led to an improved nanocomposite foam structure compared with those prepared in the presence of SDBS.

TEM micrographs (Figure 5) of the SDOSS-synthesized foam containing 0.3 wt % SWCNTs indicated the incorporation of SWCNTs in the polymeric matrix. As the aqueous phase was added to the organic phase, the water-soluble surfactant was adsorbed on the w/o interface stabilized by Span80. The competition between the water-soluble and oil-soluble surfactants to migrate to the interface may have isolated some surfactant molecules from the surface of the SWCNTs. As a result, hydrophobic SWCNTs, especially those detached from the surfactant molecules, tended to enter the organic phase. A comparison of the TEM micrographs of SDOSS and F127-syntheized nanocomposite foams revealed that the F127-stabilized SWCNTs were more likely to enter the organic phase compared with those stabilized by SDOSS.

Interestingly, the SDOSS-synthesized nanocomposite foams with an improved morphology were electrically conductive. Figure 6 shows the electrical conductivity of the nanocomposite foams prepared with the SDOSS surfactant versus the SWCNT levels. As shown, the electrical conductivities of the foams prepared with both the anionic SDOSS and SDBS surfactants were almost identical. The changes in the electrical conductivity of the nanocomposite foams could have been connected to the percolation model; this indicated the formation of a conducting network on/in the voids' wall. However, the discrepancy with the theoretical value ($\alpha = 2$, α is a parameter determined by the special
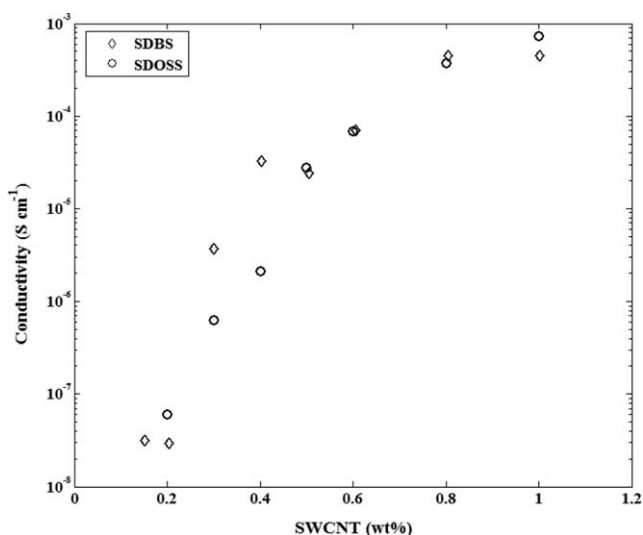

Figure 6. Electrical conductivities of the SDOSS- and SDBS-synthesized polyHIPE nanocomposite foams versus SWCNT levels.
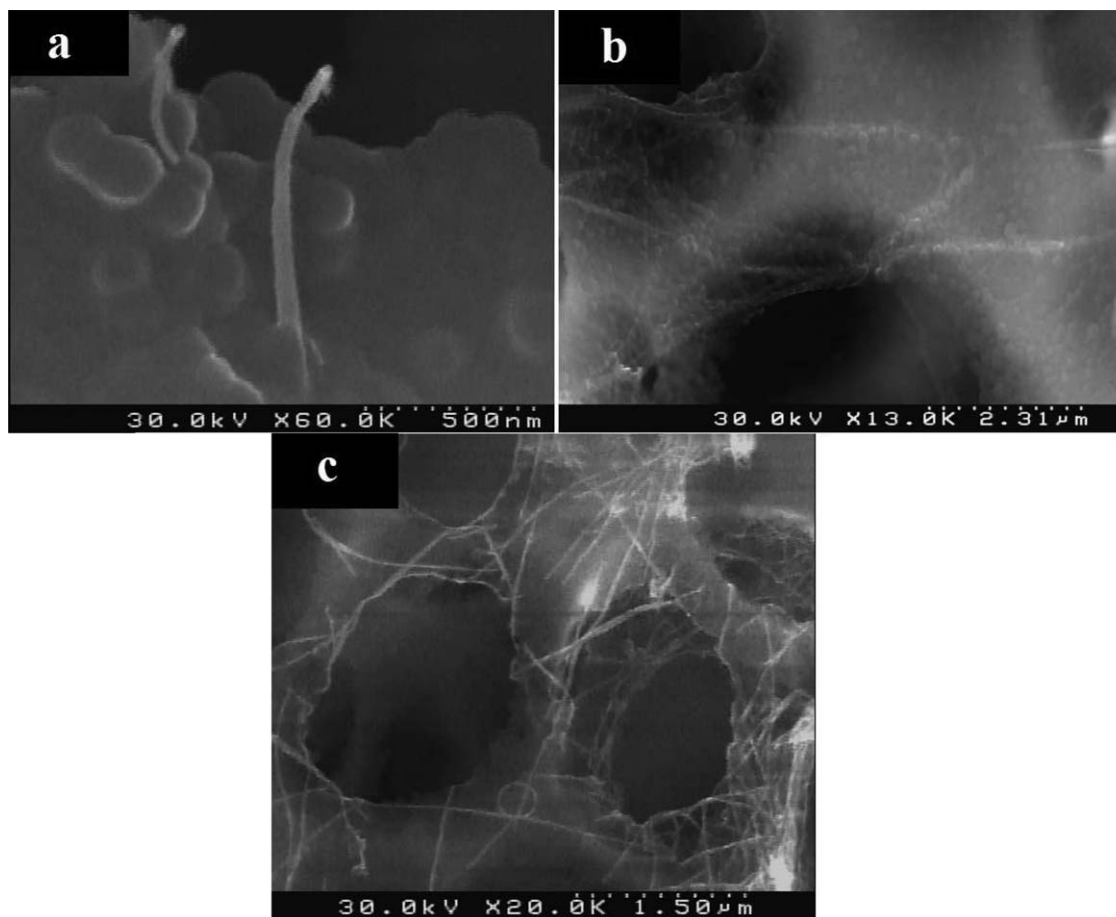
Figure 7. FESEM micrographs of the SDOSS-synthesized nanocomposite foams containing various SWCNT levels: (a) 0.3, (b) 0.8, and (c) 1 wt %

arrangement of SWCNTs) may have indicated the formation of a nongeometric conducting network and, consequently, the introduction of tunneling between the adjacent nanotubes as the dominant conductivity mechanism. At SWCNT contents below 0.2 wt %, the distance between the nanotubes may have been so large that the polymeric matrix controlled the transport of electrical charges. In this case, the electrical resistance of the composite foam was fairly close to that of the poly(styrene-*co*-divinylbenzene) matrix. The conducting fillers and insulating gaps between them could be considered capacitors. Therefore, the insulating gaps were so large that the chance to transport the electrical charges between the adjacent SWCNTs was very low. Because the constrained charges of the polymeric matrix belonged to the valence band, the whole composite foam acted as an insulator (Figure 6).

As the SWCNT level increased above 0.2 wt %, the insulator gap between the neighboring nanotubes decreased. When the average distance of the nanotubes became less than 1.8 nm, the tunneling length of electrons, hopping, and tunneling become the main mechanisms for electron transport. In this case, a strong electric field was likely to be induced within the narrow insulating gaps between the conducting nanofillers. As a result, the free electrons of the conducting SWCNTs gained sufficient energy to tunnel over the insulating gaps.[28] With the addition of more conducting SWCNTs to the polymeric matrix, the

nanotubes became much closer, and the first conducting path was formed at the percolation threshold. Because of direct contact of SWCNTs in the percolation region, the electrical charges
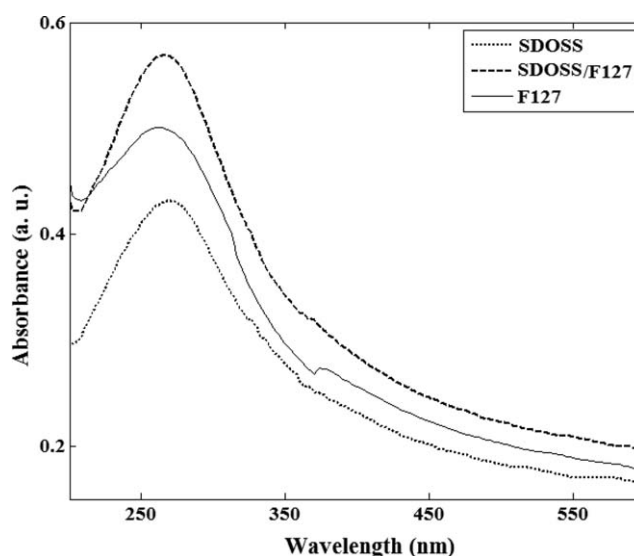

Figure 8. UV–vis spectra of 0.05 wt % SWCNT aqueous dispersions prepared with SDOSS, F127, and the SDOSS/F127 mixed surfactant.
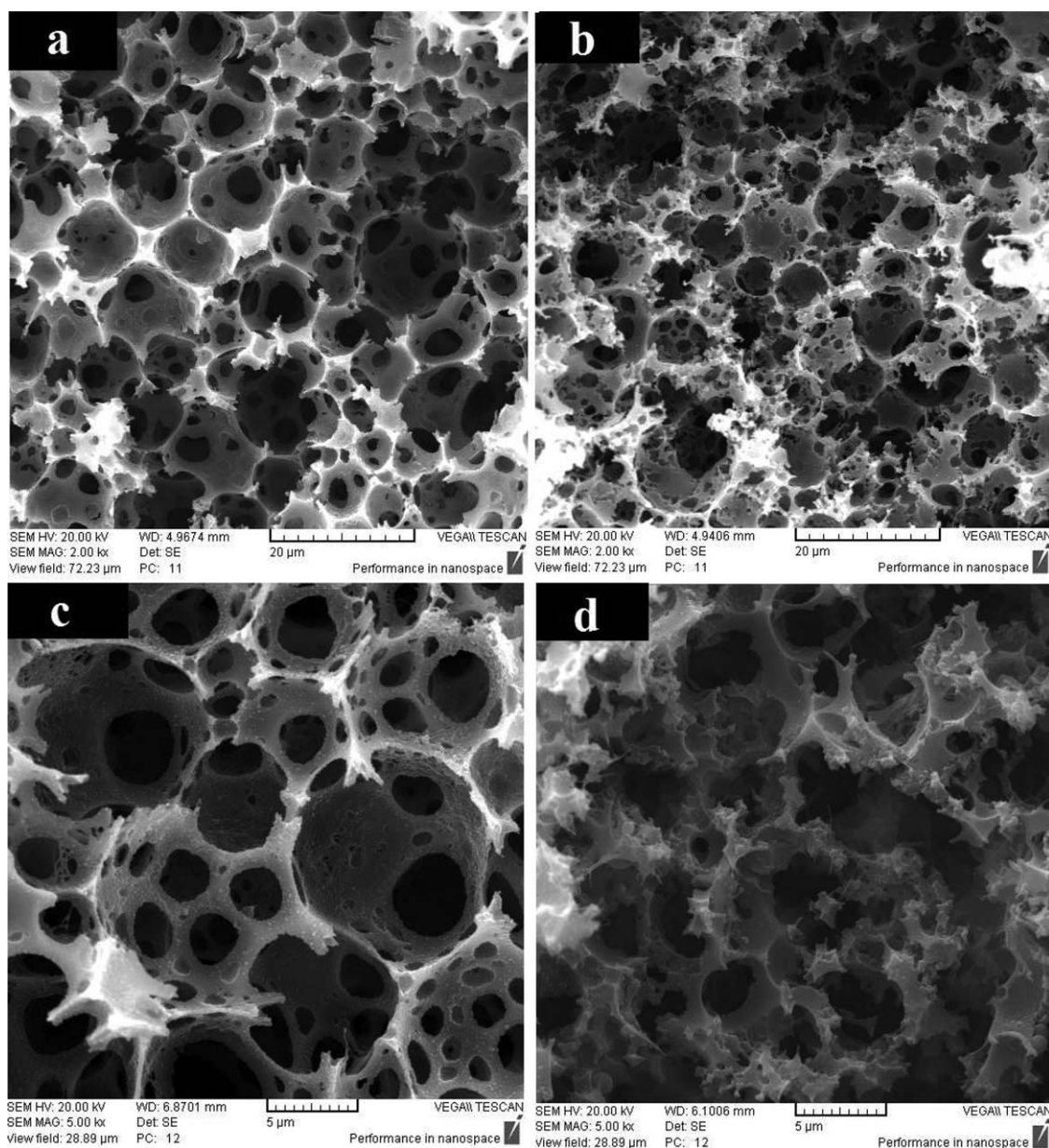
Figure 9. SEM micrographs of nanocomposite foams prepared with different surfactants and SWCNT levels: (a) SDOSS/F127 and 0.3 wt % SWCNTs, (b) SDOSS and 0.3 wt % SWCNTs, (c) SDOSS/F127 and 1 wt % SWCNTs, and (d) SDOSS and 1 wt % SWCNTs.

of the conducting filler played a major role in the electrical conductivity of the nanocomposite foam. Because the free charges belonged to the conduction band, the electrical conductivity of the composite foam increased by several orders of magnitude in the percolation region (Figure 6). With a further increase in the SWCNT content above 0.8 wt %, the electrical conductivity remained almost constant, despite the formation of a three-dimensional network within the nanocomposite foam. This was presumably due to a significant loss in the electric current at contact points (contact resistance), and this led to a plateau in the percolation region.[15,16]

The FESEM micrographs (Figure 7) showed the dispersion state and orientation of nanotubes in the polyHIPE nanocomposites containing various SWCNT levels. It was likely that the growing

polymeric layer grafted onto the surface of the SWCNTs and engulfed them, especially at low SWCNT levels. In this case, although the presence of SWCNTs as pins at the fractured cross section was obvious [Figure 7(a)], the nanotubes were not observed on the polyHIPE wall surface. As the SWCNT level increased to 0.8 wt %, some SWCNTs migrated to the organic phase and were located near the interface because of the removal of surfactant molecules from the nanotube surface [Figure 7(b)]. As shown, the nanotubes formed a network on the surface of the polyHIPE foam containing 1 wt % SWCNTs [Figure 7(c)]. With a further increase in the SWCNT concentration, the migration of nanotubes from the aqueous phase to the organic phase was restricted because of the saturation of the layer adjacent to the interface between the phases. Therefore, a
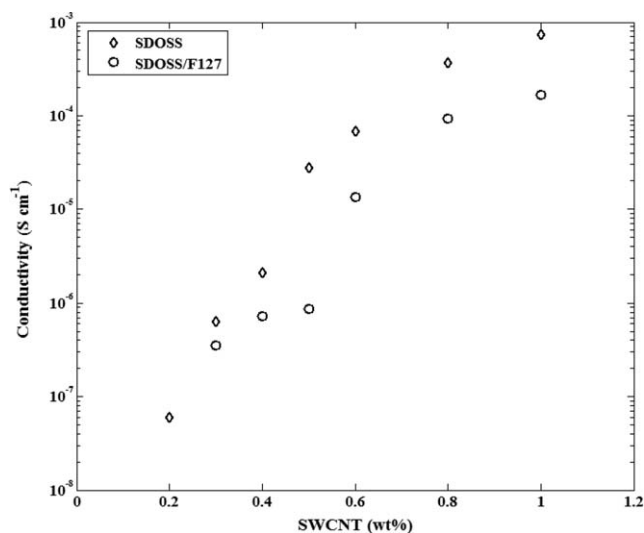
Figure 10. Electrical conductivities of nanocomposite foams prepared with SDOSS and the SDOSS/F127 mixed surfactant versus SWCNT levels.

large portion of the SWCNTs remained dispersed in the aqueous phase and precipitated onto the resulting polyHIPE wall surface during the polymerization and drying processes.

The electrical conductivity of the nanocomposite foam arose from the formation of conducting networks within the polymeric matrix or on the surface of the polyHIPE nanocomposite foam. Furthermore, sulfate ions (S_3^-) of the SDOSS molecules may have acted as charge carriers and contributed to electron transport between the adjacent SWCNTs. In other words, in the case where the distance between the nanotubes in the nanocomposite foam was larger than the tunneling length of the electrons, the S_3^- ions played a dominant role in charge transport and conductivity improvement.

SDOSS/F127-Synthesized polyHIPE/SWCNT Foams

As previously mentioned, the nanocomposite foams prepared with the block copolymer F127 preserved the conventional microstructure of the polyHIPEs without showing any electrical conductivity. With the individual roles of F127 and SDOSS in the proper dispersion of the SWCNTs and the electrical conductivity of the nanocomposite foam, the SDOSS/F127 mixed-surfactant system was used to disperse SWCNTs in the aqueous phase of the HIPEs. Figure 8 shows the UV–vis spectra of 0.05 wt % SWCNTs aqueous dispersions prepared with SDOSS, F127, and SDOSS/F127 mixed surfactant. The peaks appeared in the spectra of SWCNT dispersions in various media can give information on the structure of nanotubes with different diameters. The peak appearing at 273 nm in all three cases was attributed to isolated nanotubes or small bundles because of the surface excitation of electrons.[32,33] The UV–vis absorption intensity could be used as a criterion for the dispersion quality of SWCNTs. As shown, the SDOSS/F127 mixed surfactant showed a stronger absorption intensity, presumably because of the more effective roles of F127 and SDOSS in the dispersion of nanotubes in the aqueous phase to overcome attractive van der Waals forces between the SWCNT bundles. According to the spectra, the SDOSS/F127 surfactant mixture led to the more

effective dispersion of the SWCNTs compared with those of the SDOSS and F127 ones separately.

It seemed that the co-adsorption of long F127 and charged SDOSS molecules on the surface of the SWCNTs played a more effective role in the stability of HIPE. The F127 and SDOSS molecules stabilized the SWCNTs in the aqueous phase, respectively, through electrical repulsion and steric hindrance. Because both surfactants were simultaneously added to the aqueous phase, a number of SDOSS molecules were likely to form copolymer chains with polyelectrolyte properties through van der Waals interactions with the PPO blocks of F127 chains.

Figure 9 shows the SEM micrographs of polyHIPE nanocomposite foams containing 0.3 and 1 wt % SWCNTs prepared with SDOSS and SDOSS/F127 mixed surfactants. As shown, the effective dispersion of the nanotubes with the mixed surfactant improved the microstructure of the resulting nanocomposite foams, especially for the nanocomposites with the higher SWCNT level [Figure 9(c,d)]. In this case, the nanocomposite foam prepared with SDOSS/F127 exhibited more clear open cells and windows when compared with the nanocomposite foam prepared with SDOSS. These microstructural changes could be attributed to the effective role of long chains of the block copolymer in the stabilization of SWCNTs in the aqueous phase. The PEO blocks of F127 seemed to be expanded in the aqueous phase to prevent SWCNTs from agglomeration through steric interactions.[27] In addition, negatively charged SDOSS molecules adsorbed on the PPO blocks stabilized the nanotubes by electrical repulsion. The surfactant mixture stabilized the SWCNTs in the aqueous phase of the HIPEs through electrosteric repulsion.

Figure 10 shows the electrical conductivity variation of the SDOSS/F127-synthesized nanocomposite foams versus the SWCNT levels. The electrical conductivities of the SDOSS/F127-synthesized foams were lower than those prepared with the anionic surfactant, that is, SDOSS. More importantly, the SDOSS/F127-synthesized foams showed reasonable conductivity values as compared with the insulating F127-synthesized nanocomposite foams. The electrical conductivity of the foams prepared with the mixed-surfactant system could be partly attributed to the electrical charges of the anionic SDOSS surfactant. The negative charges of S_3^- distributed between the nonionic F127 chains acted as charge carriers and facilitated the electrical current between the adjacent SWCNTs. The lower electrical conductivities of the SDOSS/F127-synthesized nanocomposite foams compared with the SDOSS-synthesized ones was presumably due to the lower density of S_3^- and the higher thickness of the insulating layer around the SWCNTs; this led to a lower efficiency of electron tunneling between the adjacent SWCNTs.[28]

CONCLUSIONS

PolyHIPE nanocomposite foams containing various SWCNT contents were successfully prepared with different anionic, cationic, and mixed surfactants to disperse the nanotubes in the aqueous phase of HIPEs. The effects of the surfactant type on the microstructure and electrical conductivity of the resulting nanocomposite foams were investigated. The microstructure and electrical conductivity of the SDBS-synthesized foams were

improved compared with those of the nanocomposite foams prepared with the anionic SDS surfactant. However, the resulting foams did not resemble the typical polyHIPE foam microstructure because of the migration of some SDBS molecules from the surface of the SWCNTs to the interface of the two phases and, consequently, the partial instability of the HIPEs. Although the use of the F127 and CTAB/SDBS surfactant systems resulted in a reasonable open-cellular polyHIPE structure, all of the nanocomposite foams were electrical insulators. This behavior was connected to the grafting of insulating poly(styrene-*co*-divinylbenzene) chains on the surface of the SWCNTs and, therefore, the lack of an effective electrical contact between the adjacent SWCNTs to conduct the electric current through hopping and tunneling mechanisms. Surprisingly, the use of SDOSS with a Gemini-like structure significantly improved both the microstructural and electrical characteristics of the resulting nanocomposite foams. This behavior was attributed to the stronger interactions of SDOSS molecules with the SWCNTs and, thereby, the lower migration rate of surfactant molecules to the interface. The results show that HLB as one of the main characteristics could not be the only criterion to select a suitable aqueous-phase surfactant, whereas the chemical structure of the surfactant and its interactions with SWCNTs exhibited a greatly important role. Although SDS and SDOSS had high HLB values, the former destabilized the HIPE, whereas the latter resulted in an interconnected open-cellular solid foam because of its effective interactions with the SWCNTs. The use of the SDOSS/F127 mixed surfactant caused a significant improvement in the foam microstructure. However, the electrical conductivity of the foams decreased to some extent compared to that of the SDOSS-synthesized composite foams; this was presumably due to an increase in the tunneling length of electrons between the adjacent SWCNTs.

REFERENCES

1. Kazukauskas, V.; Kalendra, V.; Bumby, C. W.; Ludbrook, B. M.; Kaiser, A. B. *Phys. Stat. Solidi C* **2008**, *5*, 3172.

2. Shaffer, M. S. P.; Fanand, X.; Windle, A. H. *Carbon* **1998**, *36*, 1603.

3. Wu, T. M.; Lin, S. H. *J. Polym. Sci. Part A: Polym. Chem.* **2006**, *44*, 6449.

4. Wu, T. M.; Chang, H. L.; Lin, Y. W. *Compos. Sci. Technol.* **2009**, *69*, 639.

5. Jam, J. E.; Ahangari, M. *Polym. Plast. Technol. Eng.* **2012**, *51*, 1474.

6. Zhang, X.; Zhang, J.; Wang, R.; Zhu, T.; Liu, Z. *Chem. Phys. Chem.* **2004**, *5*, 998.

7. Park, C.; Ounaies, Z.; Watson, K. A.; Crooks, R. E.; Smith, J.; Lowther, S. E.; Connell, J. W.; Siochi, E. J.; Harrison, J. S.; Clair, T. L. *Chem. Phys. Lett.* **2002**, *364*, 303.

8. Ayesh, A. S. *J. Polym. Res.* **2012**, *19*, 27.

9. Zhang, X.; Zhang, J.; Liu, Z. *Carbon* **2005**, *43*, 2186.

10. Li, J.; Ma, P. C.; Chow, W. S.; To, C. K.; Tang, B. Z.; Kim, J. K. *Adv. Funct. Mater.* **2007**, *17*, 3207.

11. Ugur, S.; Yargi, O.; Pekcan, O. *Can. J. Chem.* **2010**, *88*, 267.

12. Bauhofer, W.; Kovacs, J. Z. *Compos. Sci. Technol.* **2009**, *69*, 1486.

13. Du, F.; Fischer, J. E.; Winey, K. I. *Phys. Rev. B* **2005**, *72*, 121404.

14. Yao, S. H.; Dang, Z. M.; Jiang, M. J.; Xu, H. P. *Appl. Phys. Lett.* **2007**, *91*, 212901.

15. Hermant, M. C.; Klumperman, B.; Koning, C. E. *Chem. Commun.* **2009**, *19*, 2738.

16. Hermant, M. C.; Verhulst, M.; Kyrylyuk, A. V.; Klumperman, B.; Koning, C. E. *Compos. Sci. Technol.* **2009**, *69*, 656.

17. Menner, A.; Salgueiro, M.; Shaffer, M.; Bismarck, A. *J. Polym. Sci. Part A: Polym. Chem.* **2008**, *46*, 5708.

18. Menner, A.; Verdejo, R.; Shaffer, M.; Bismarck, A. *Langmuir* **2007**, *23*, 2398.

19. Cameron, N. R. *J. Chromatogr. Libr.* **2003**, *67*, 255.

20. Silverstein, M.; Tai, H.; Sergienko, A.; Lumelsky, Y.; Pavlovsky, S. *Polymer* **2005**, *46*, 6682.

21. Sharma, A. L.; Kumar, P.; Deep, A. *Polym. Plast. Technol. Eng.* **2012**, *51*, 1382.

22. Avila-Orta, C. A.; Raudry-Lopez, C. E.; Davila-Rodriguez, M. V.; Aguirre-Figueroa, Y. A.; Cruz-Delgado, V. J.; Neira-Velazquez, M. G.; Medellin-Rodriguez, F. J.; Hsiao, B. S. *Int. J. Polym. Mater. Polym. Biomater.* **2013**, *62*, 635.

23. Dai, K.; Ji, X.; Xiang, Z.; Zhang, W.; Tang, J.; Li, Z. *Polym. Plast. Technol. Eng.* **2012**, *51*, 304.

24. Ling, J.; Zhai, W.; Feng, W.; Shen, B.; Zhang, J.; Zheng, W. *ACS Appl. Mater. Interfaces* **2013**, *5*, 2677.

25. Wenseleers, W.; Vlasov, I.; Goovarets, E.; Obraztsova, D.; Lobach, A.; Bouwen, A. *Adv. Funct. Mater.* **2004**, *14*, 1105.

26. Sadeghi, S.; Moghbeli, M. R. *Colloid Surf. A* **2012**, *409*, 42.

27. Litt, M. H.; Hsieh, B. R.; Krieger, I. M.; Chen, T. T.; Lu, H. L. *J. Colloid Interface Sci.* **1987**, *115*, 312.

28. Bao, W. S.; Meguid, S. A.; Zhu, Z. H.; Weng, G. J. *J. Appl. Phys.* **2012**, *111*, 093726.

29. Barbetta, A.; Cameron, N. R. *Macromolecules* **2004**, *37*, 3202.

30. Karimian, H.; Moghbeli, M. R. *Polym. Plast. Technol. Eng.* **2014**, *53*, 344.

31. Crescenzo, A.; Germani, R.; Canto, E.; Giordani, S.; Savelli, G.; Fontana, A. *Eur. J. Org. Chem.* **2011**, *2011*, 5641.

32. Matarredona, O.; Rhoads, H.; Li, Z.; Harwell, J.; Balzano, L.; Resasco, D. *J. Phys. Chem. B* **2003**, *107*, 13357.

33. Grossiord, N.; Regev, O.; Loos, J.; Meuldijk, J.; Koning, C. E. *Anal. Chem.* **2005**, *77*, 5135.